

Supplementary Information

Redox-catalysis flow electrode desalination in an organic solvent

Qiang Wei^{1,2}, Lufan Tang^{1,2}, Karthick Ramalingam^{1,2}, Mengjun Liang^{1,2}, Jinxing Ma³, Yumeng Shi⁴, Kwun Nam Hui⁵, Kwan San Hui⁶, Fuming Chen^{1,2*}

¹ *Guangdong Provincial Key Laboratory of Quantum Engineering and Quantum Materials, Guangdong Engineering Technology Research Center of Efficient Green Energy and Environment Protection Materials, School of Physics and Telecommunication Engineering, South China Normal University, Guangzhou 510006, China fmchen@m.scnu.edu.cn*

² *School of Electronics and Information Engineering, South China Normal University, Foshan, 528225, China*

³ *Key Laboratory for City Cluster Environmental Safety and Green Development of the Ministry of Education, Institute of Environmental and Ecological Engineering, Guangdong University of Technology, Guangzhou, 510006, China*

⁴ *International Collaborative Laboratory of 2D Materials for Optoelectronics Science and Technology of Ministry of Education, Institute of Microscale Optoelectronics, Shenzhen University, Shenzhen 518060, P. R. China*

⁵ *Joint Key Laboratory of the Ministry of Education, Institute of Applied Physics and Materials Engineering, University of Macau, Avenida da Universidade, Taipa, Macau SAR 999078, China*

⁶ *School of Engineering, Faculty of Science, University of East Anglia, Norwich NR4 7TJ, United Kingdom*

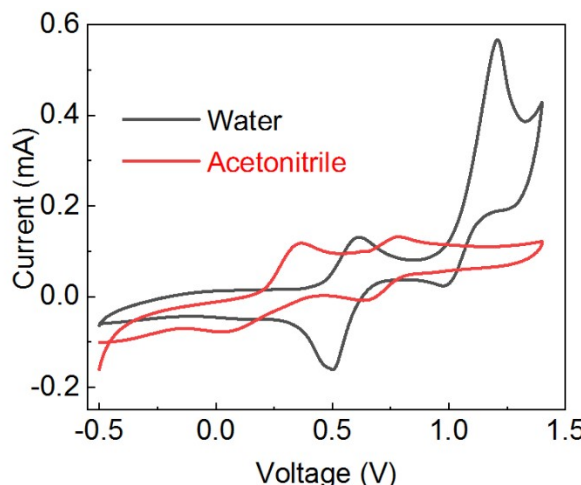


Figure S1. Three-electrode CV of I^-/I^{3-} solution with Pt counter and Ag/AgCl reference in acetonitrile or water medium

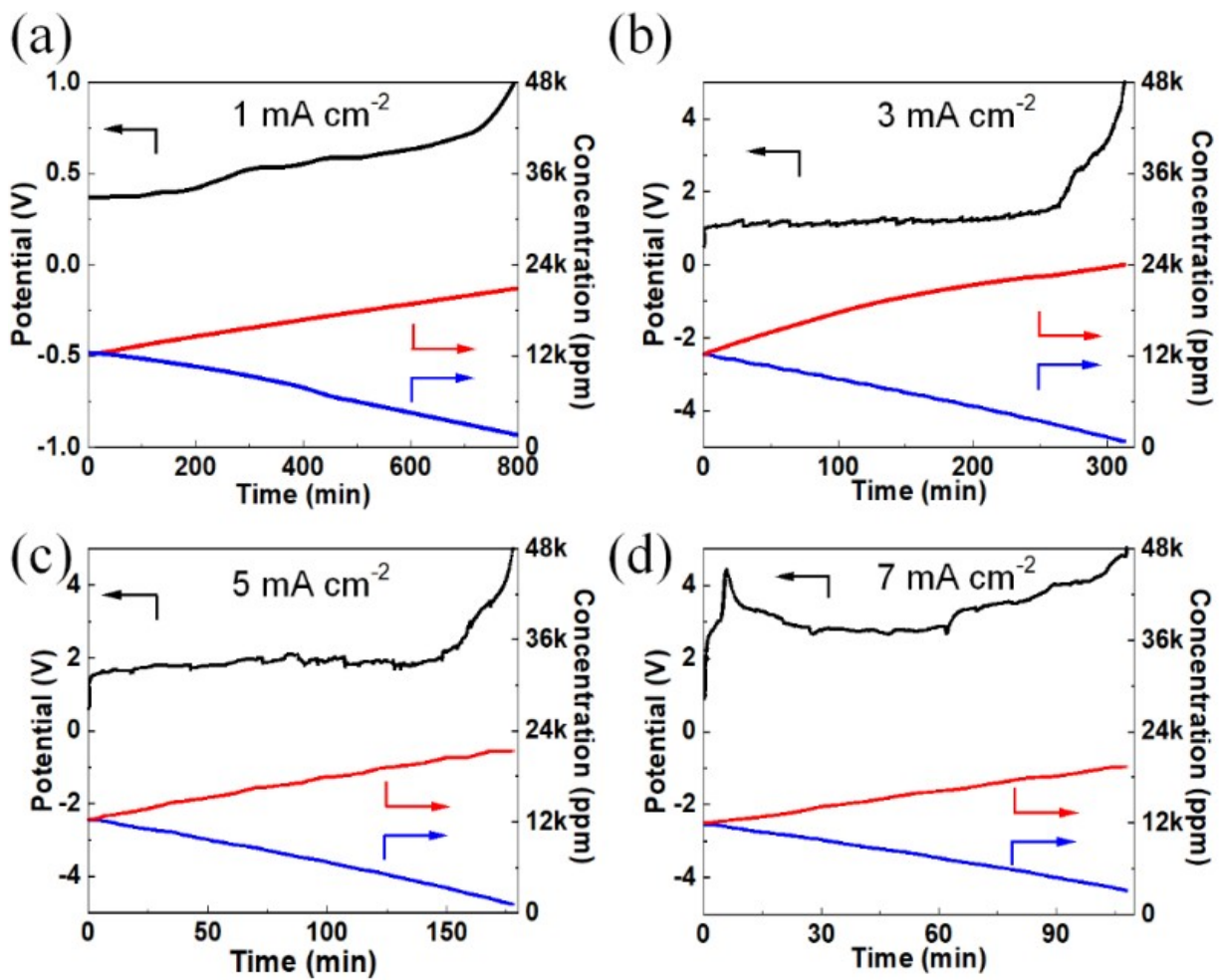


Figure S2. The desalination performance at different current densities from Figure 1: (a) 1 mA cm^{-2} ; (b) 3 mA cm^{-2} ; (c) 5 mA cm^{-2} ; (d) 7 mA cm^{-2} . The initial salt feed: 12000 ppm salt. Electrolyte: 50 mM NaI/30 mM I₂ and 500 mM TBAP in 5 ml acetonitrile; salt feed: 12000 ppm in 3 mL. The red solid lines represent the conductivity of the brine stream while the blue solid lines the conductivity of the desalinated stream.

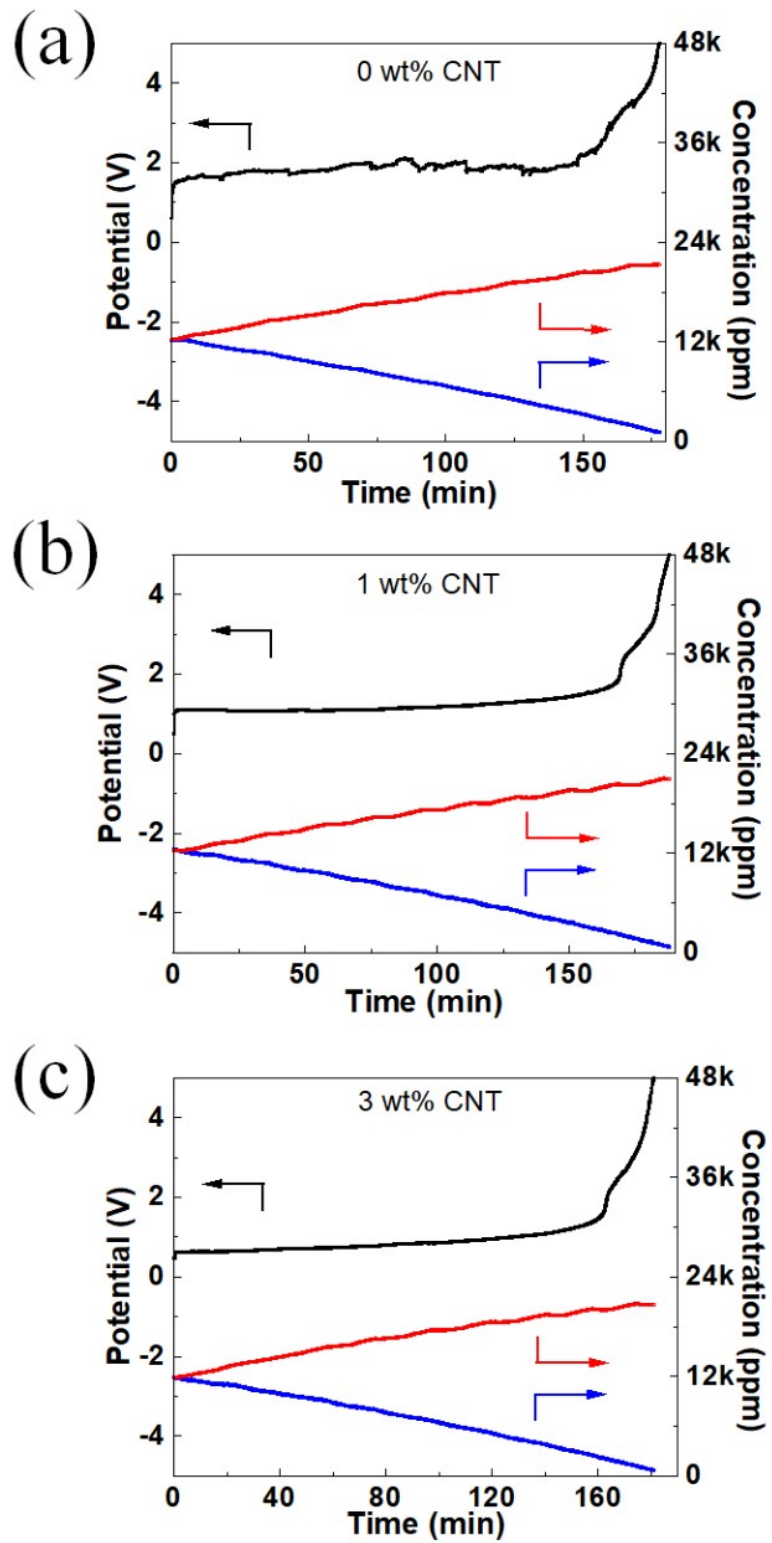


Figure S3. The desalination performance of different CNTs content with the ratio of 0 wt% (a), 1 wt% (b), 3 wt% (c). The initial salt feed: 12000 ppm salt, current density: 5 mA cm^{-2} ; The initial salt feed: 12000 ppm salt. Electrolyte: 50 mM NaI/30 mM I₂ and 500 mM TBAP in 5 ml acetonitrile; salt feed: 12000 ppm in 3 mL; Current density: 5 mA cm^{-2} . The red solid lines represent the conductivity of the brine stream while the blue solid lines the conductivity of the desalinated stream.

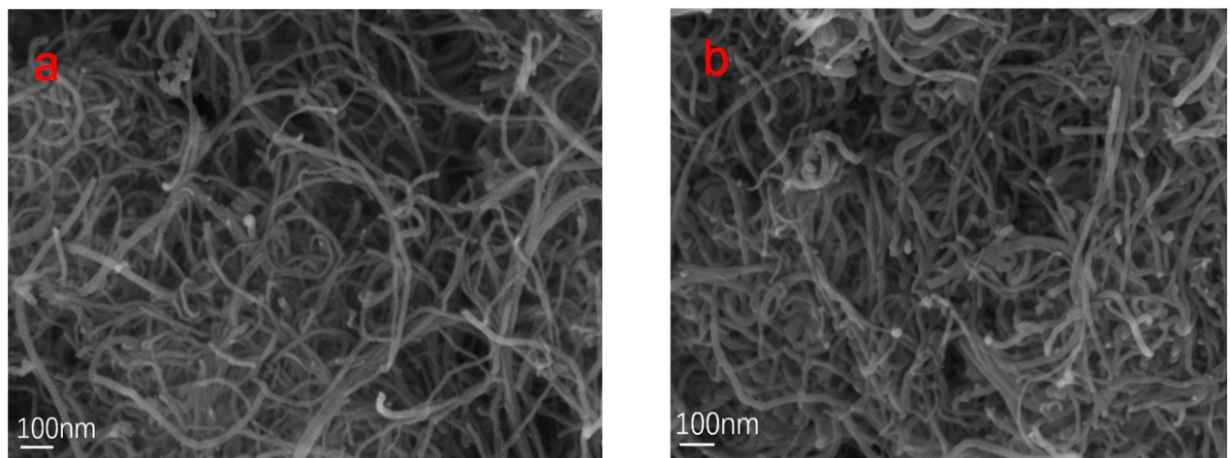


Figure S4. SEM images of multi wall carbon nanotubes, before (a) and after (b) the desalination test. The current density: 5 mA cm^{-2} .

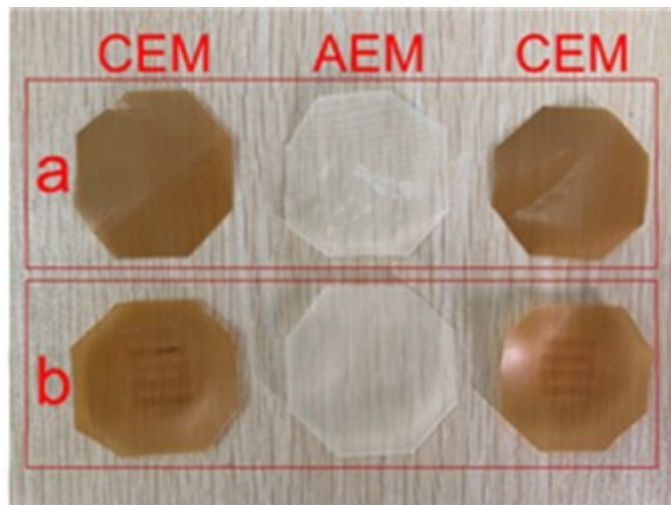


Figure S5. Membrane images before (a) and after (b) the desalination test.

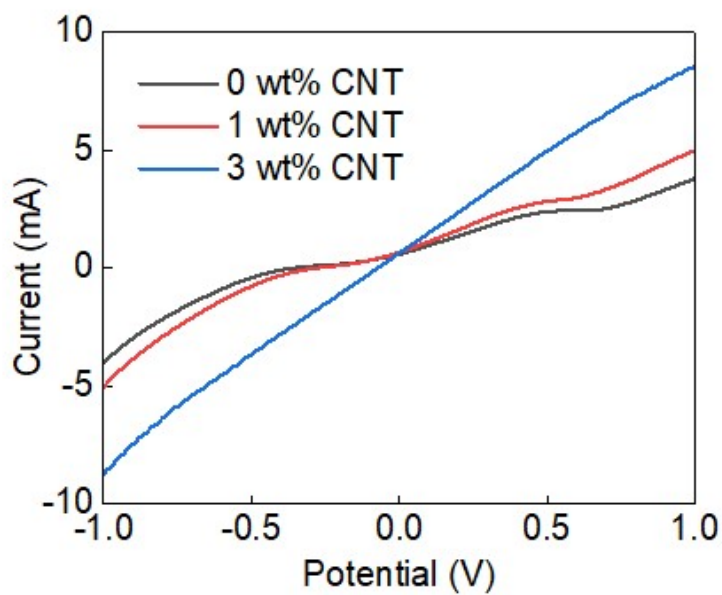


Figure S6. The LSV curve of two-electrode architecture in organic redox flow electrode. Device structure: end plate | graphite paper as current collector | redox couples/carbon flow chamber || redox couples/carbon flow chamber | graphite paper as the current collector | end plate (The symbols of | and || denote the compartment separation and membrane, respectively.) The redox couples/carbon flow chamber were fabricated from rubber material with the dimension of 17 mm length, 4 mm width, 5 mm thickness. The active area is 68 mm² totally.

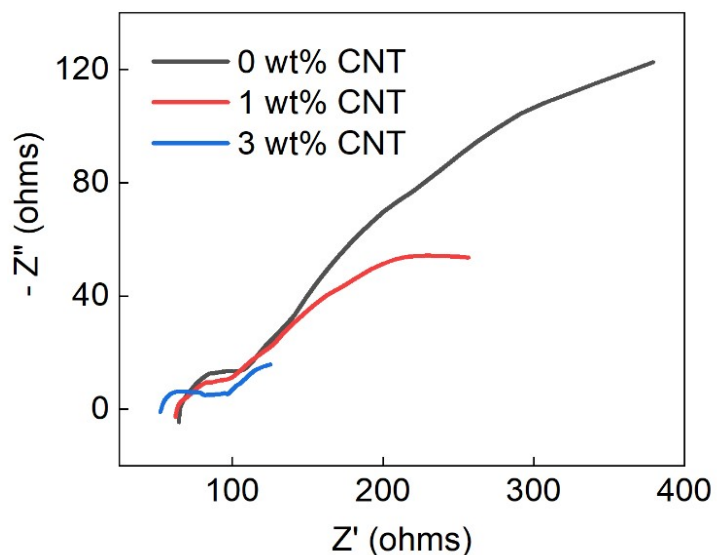


Figure S7. Nyquist plots of organic redox flow electrodes measured by two-electrode configuration, redox couples with 0, 1, 3 wt % CNTs measured under the zero-bias with the frequency range between 100 kHz to 10 mHz at a sinusoidal amplitude of 10 mV.

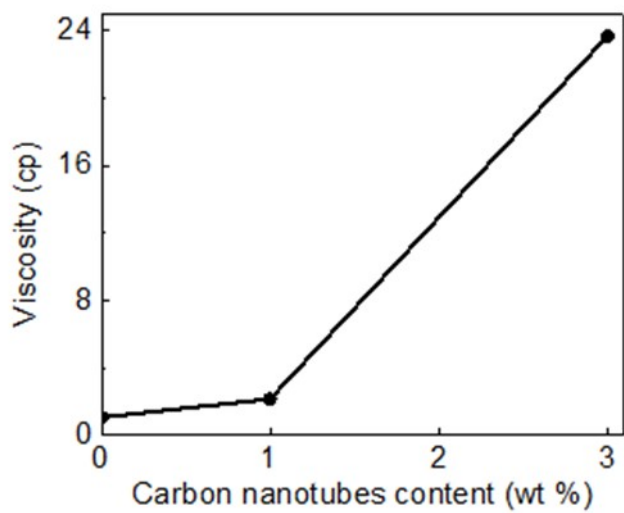


Figure S8. The relationship between carbon nanotubes content and viscosity.

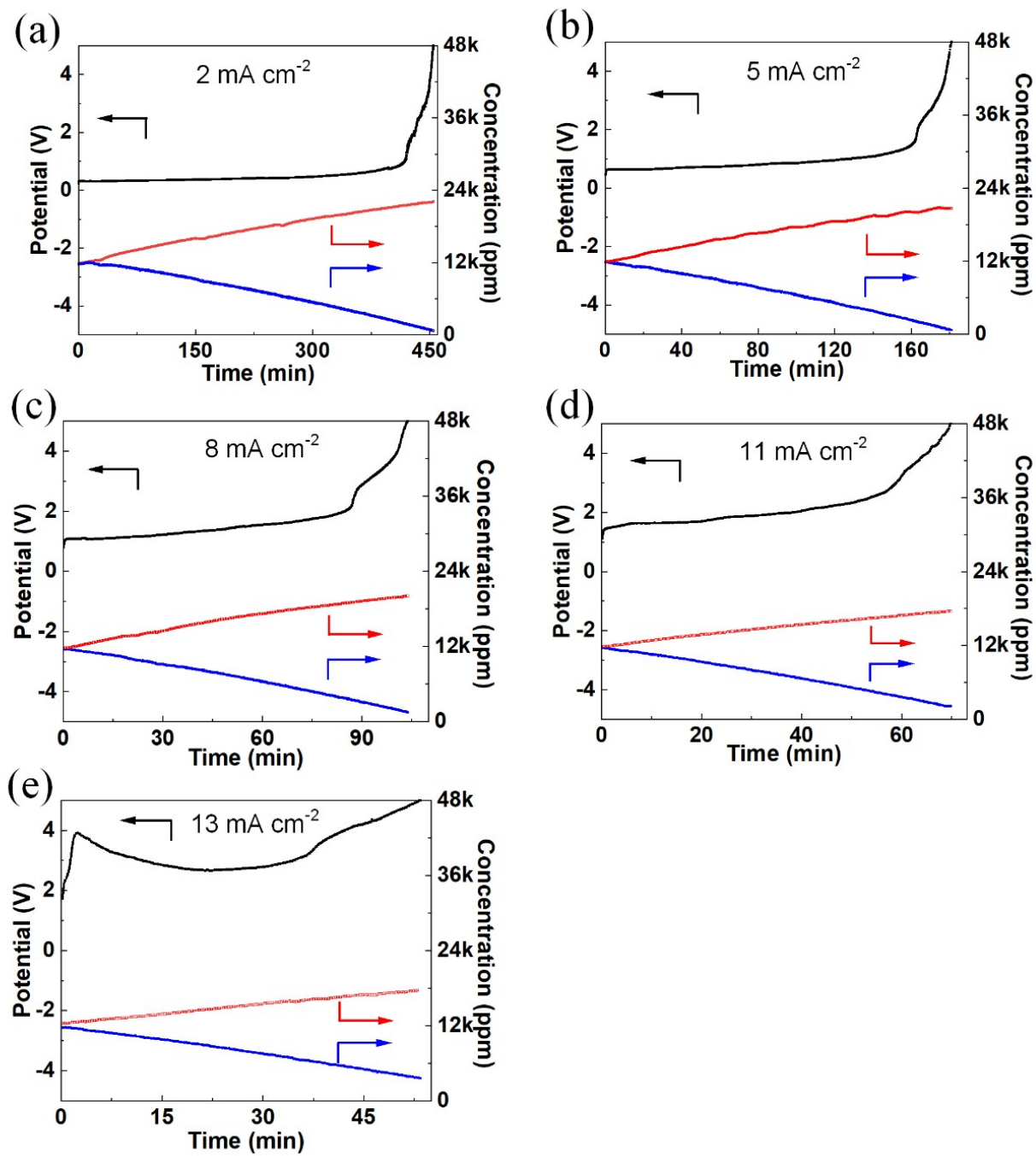


Figure S9. The desalination performance at different current densities: (a) 2 mA cm^{-2} ; (b) 5 mA cm^{-2} ; (c) 8 mA cm^{-2} ; (d) 11 mA cm^{-2} ; (e) 13 mA cm^{-2} . The initial salt feed: 12000 ppm salt in 3 mL; CNTs content: 3 wt%; Electrolyte: 50 mM NaI/ 30mM I₂ and 500 mM TBAP in 5 ml acetonitrile. The red solid lines represent the conductivity of the brine stream while the blue solid lines the conductivity of the desalinated stream.

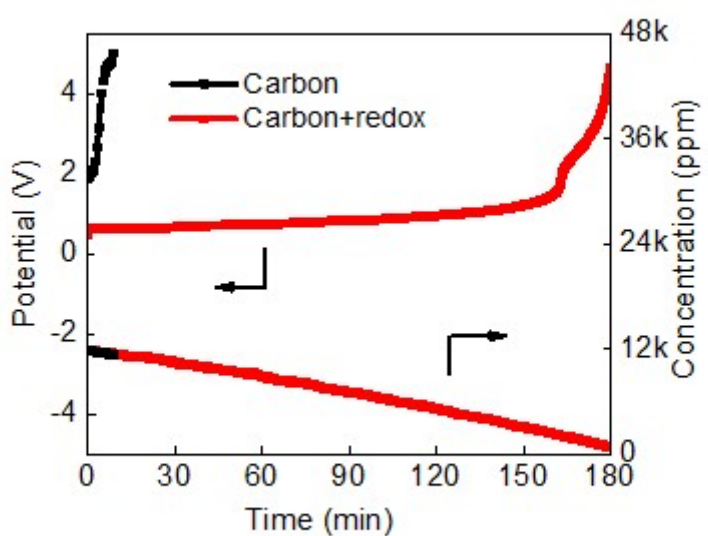


Figure S10 The comparison of desalination performance with/without the addition of the redox couples. The constant current density: 5 mA cm⁻².

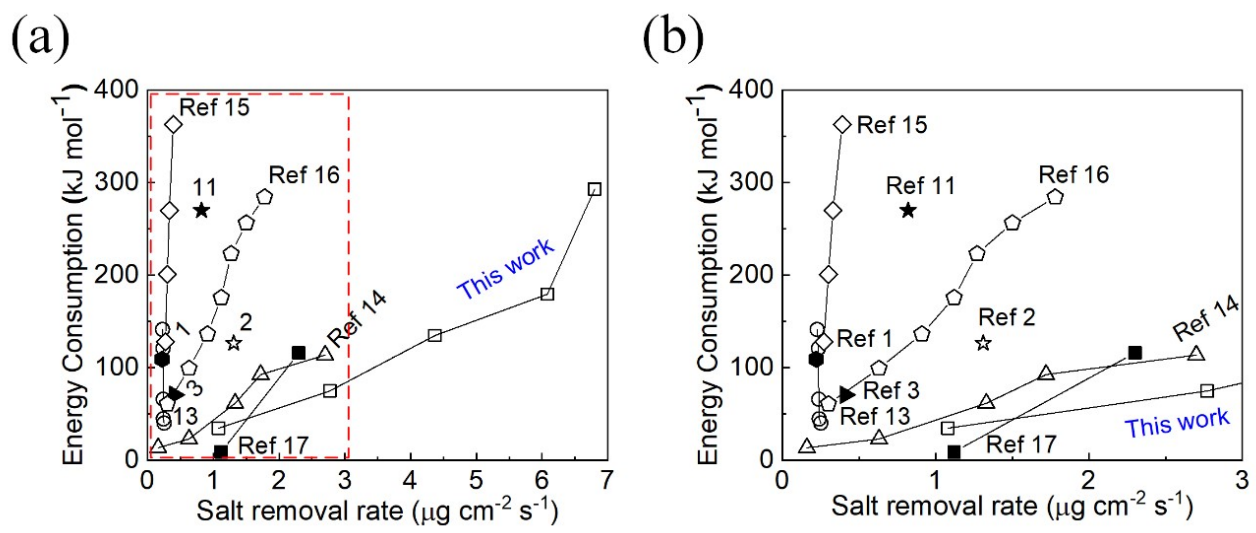


Figure S11. The comparison plot of salt removal rate vs consumption extracted from Table S1.

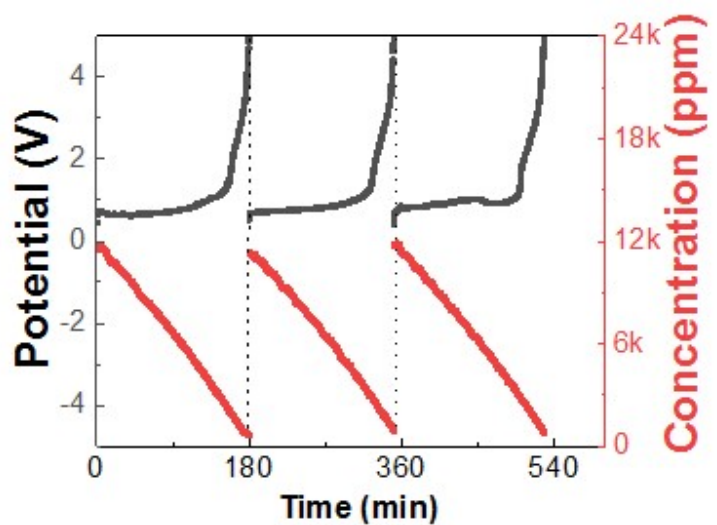


Figure S12. Results of multi-cycle test of the current desalination system with 3 % CNTs and 50 mM NaI /30 mM I₂ at the current density of 5 mA cm⁻² without the replacement of electrode materials and membranes.

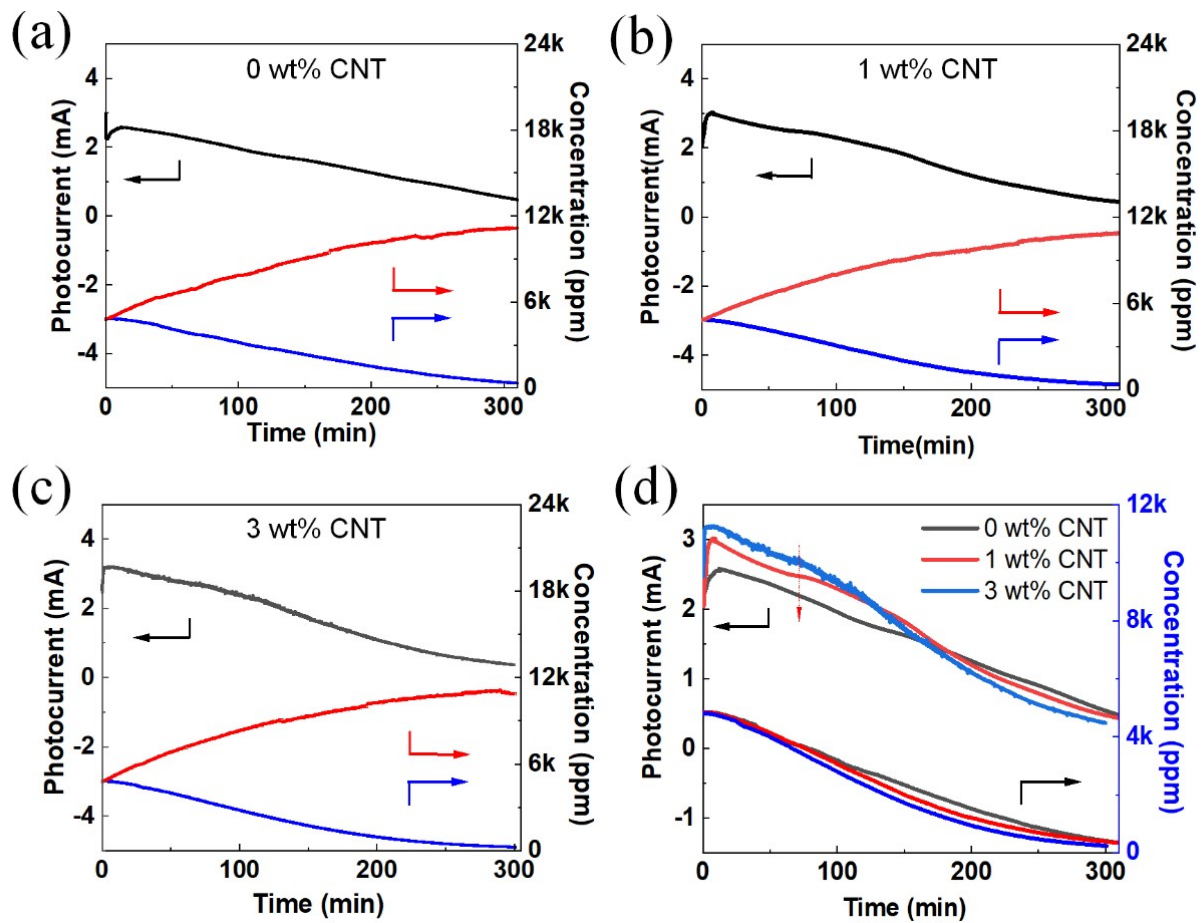


Figure S13. The organic redox flow desalination driven by solar light at zero bias (short circuit): (a) 0 wt% CNT; (b) 1 wt% CNT; (c) 3 wt% CNT; (d) the overlapping curves of 0, 1, 3 wt% CNT. The initial salt feed: 6000 ppm in 3 mL.

Supplementary Table S1. Comparison of FCDI energy consumption and salt removal rate

Electrode materials	Carbon content	Salt feed (ppm)	Operation voltage or current	Salt removal rate ($\mu\text{g s}^{-1} \text{cm}^{-2}$)	Energy consumption (kJ mole $^{-1}$)	Ref.
Porous carbon	10 %	1170	3.84 mA cm $^{-2}$	0.22	109.1	1
YP-50F activated carbon	13%	10000	3.0 mA cm $^{-2}$	1.31	126.4	2
Modified AC	10 %	1000	1.43 mA cm $^{-2}$	0.41	70.7	3
		200		0.17		
		1100		0.67		
Activated carbon	5%	5900	1.2 V	3.17	-	4
		14200		3.67		
		35000		5.67		
	10%			0.31		
Activated carbon	15%	5800	1.2 V	0.42	-	5
	20%			0.67		
Activated carbon-N and Activated carbon-S	35%	35000	1.2 V	~33.13	-	6
Carbon black	2.5%	1000	1.2 V		~125	7
Activated carbon, carbon black	5%	5800	1.2 V	0.86	-	8
				0.76		
Activated carbon, carbon black	10%	2000	1.15 mA cm $^{-2}$	0.71	-	9
				0.68		
Activated carbon, carbon black	5.72%	10000	2.8 V	1.83	-	10
CNTs suspension	7.41 %	11688	1.6 V	0.82	270.0	11
Activated carbon, and FCNTs	5.25%	35000	1.2 V	33.43	-	12

V ²⁺ /V ³⁺						
Activated carbon (AC)				0.226	192.89	
				0.235	168.66	
AC and V ²⁺ /V ³⁺	7.41%	3000	0.43 mA cm ⁻²	0.237	103.26	13
AC, V ²⁺ /V ³⁺ and 0.5% CNTs				0.24	77.99	
AC, V ²⁺ /V ³⁺ and 1% CNTs				0.25	72.62	
			0.47 mA cm ⁻²	0.16	40.95	
Activated carbon, carbon black, ferri- /ferrocyanide	10 %	9000	1.42 mA cm ⁻²	0.63	52.2	
			2.38mA cm ⁻²	1.33	98.07	14
			3.33mA cm ⁻²	1.72	135.0	
			4.28 mA cm ⁻²	2.7	160.0	
			0.4 mA cm ⁻²	0.27	177.0	
TE-3 activated carbon beads	8.3 %	1170	0.52 mA cm ⁻²	0.3	263.5	15
			0.6 mA cm ⁻²	0.33	345.6	
			0.8 mA cm ⁻²	0.39	456.0	
			0.573 mA cm ⁻²	0.3	97.3	
			1.146 mA cm ⁻²	0.63	142.8	
			1.719 mA cm ⁻²	0.91	187.0	
DARCO, and Noritactivated charcoal	2000	10 %	2.292 mA cm ⁻²	1.12	233.7	16
			2.865 mA cm ⁻²	1.27	289.9	
			3.438 mA cm ⁻²	1.5	329.5	
			4.011 mA cm ⁻²	1.78	362.7	
DARCO, and Noritactivated charcoal	1000	10 %	0.909 mA cm ⁻²	1.12	35.79	
			1.818 mA cm ⁻²	2.30	162.61	17
			2 mA cm ⁻²	1.08	66.08	
			5 mA cm ⁻²	2.77	113.84	
NaI/I ₂ and 3% CNTs	3%	12000	8 mA cm ⁻²	4.37	185.13	This work
			11 mA cm ⁻²	6.08	238.07	
			13 mA cm ⁻²	6.80	373.07	

References:

1. R. Zhao, P. M. Biesheuvel and A. van der Wal, *Energy & Environmental Science*, 2012, 5.
2. K. B. Hatzell, M. C. Hatzell, K. M. Cook, M. Boota, G. M. Housel, A. McBride, E. C. Kumbur and Y. Gogotsi, *Environ Sci Technol*, 2015, 49, 3040-3047.
3. J. H. Choi and D. J. Yoon, *Water Res*, 2019, 157, 167-174.
4. S.-i. Jeon, H.-r. Park, J.-g. Yeo, S. Yang, C. H. Cho, M. H. Han and D. K. Kim, *Energy & Environmental Science*, 2013, 6, 1471.
5. S. Porada, D. Weingarth, H. V. M. Hamelers, M. Bryjak, V. Presser and P. M. Biesheuvel, *Journal of Materials Chemistry A*, 2014, 2, 9313.
6. H.-r. Park, J. Choi, S. Yang, S. J. Kwak, S.-i. Jeon, M. H. Han and D. K. Kim, *RSC Advances*, 2016, 6, 69720-69727.
7. J. Ma, C. Zhang, F. Yang, X. Zhang, M. E. Suss, X. Huang and P. Liang, *Environmental science & technology*, 2020, 54, 1177-1185.
8. X. Xu, M. Wang, Y. Liu, T. Lu and L. Pan, *ACS Sustainable Chemistry & Engineering*, 2016, 5, 189-195.
9. C. He, J. Ma, C. Zhang, J. Song and T. D. Waite, *Environ Sci Technol*, 2018, 52, 9350-9360.
10. J. Chang, F. Duan, H. Cao, K. Tang, C. Su and Y. Li, *Desalination*, 2019, 468, 114080.
11. K. Tang, S. Yiakoumi, Y. Li and C. Tsouris, *ACS Sustainable Chemistry & Engineering*, 2019, 7, 1085-1094.
12. Y. Cho, C. Y. Yoo, S. W. Lee, H. Yoon, K. S. Lee, S. Yang and D. K. Kim, *Water Res*, 2019, 151, 252-259.
13. Z. Wang, Y. Hu, Q. Wei, W. Li, X. Liu and F. Chen, *The Journal of Physical Chemistry C*, 2021, 125, 1234-1239.
14. Q. Wei, Y. Hu, J. Wang, Q. Ru, X. Hou, L. Zhao, D. Y. W. Yu, K. San Hui, D. Yan, K. N. Hui and F. Chen, *Carbon*, 2020, 170, 487-492.
15. G. J. Doornbusch, J. E. Dykstra, P. M. Biesheuvel and M. E. Suss, *Journal of Materials Chemistry A*, 2016, 4, 3642-3647.
16. C. He, J. Ma, C. Zhang, J. Song and T. D. Waite, *Environmental science & technology*, 2018, 52, 9350-9360.
17. J. Ma, J. Ma, C. Zhang, J. Song, W. Dong and T. D. Waite, *Water Res*, 2020, 168, 115186.